J Mater Sci: Mater Electron (2015) 26:6339–6343
DOI 10.1007/s10854-015-3221-y

$Ag@Ag_2SO_4$ nanoparticles: simple microwave-assistance synthesis, characterization and its co-photocatalytic degradation of methylene blue

Zabihullah Zarghami[1] · Mahnaz Maddahfar[2] · Majid Ramezani[3]

Received: 25 March 2015 / Accepted: 18 May 2015 / Published online: 23 May 2015

Abstract In the present study, for the first time Ag-core/Ag_2SO_4-shell nanoparticles were prepared through a microwave-assisted route. Sodium dodecyl sulfate played role as surfactant and sulfur precursor to produce $Ag@Ag_2SO_4$ nanoparticles. The Ag_2SO_4 shell are uniformly coated on the whole surface of Ag nanoparticles. The obtained $Ag@Ag_2SO_4$ nanoparticles exhibited higher photocatalytic efficiency than Ag nanoparticles and the effect of Ag_2SO_4-shell was significant on the photocatalytic efficiency. Furthermore, the efficiency of $Ag@Ag_2SO_4$ nanoparticles as a co-photocatalyst for the decolorization of methylene blue using visible light irradiation has been evaluated. Moreover, a possible reaction mechanism of the formation of $Ag@Ag_2SO_4$ nanoparticles has been discussed. The as-prepared $Ag@Ag_2SO_4$ nanoparticles were extensively characterized by techniques such as XRD, SEM, TEM, DRS, and FT-IR.

1 Introduction

In the recent years, photocatalysis is going to be a promising candidate for environment and energy concern like photodegradation of organic pollutants, wastewater detoxification, dye-sensitized solar cell and etc. [1–6]. Till now, various materials have been used as semiconductor photocatalysts and among of them, TiO_2 is an appropriate and efficient choice to use owing to its well-known incomparable qualities [7–11]. Nevertheless, this semiconductor has a few major drawbacks on its photoexcitation domain includes: (1) wide band gap energy 3.2 eV, (2) possess low absorption capability especially in the visible light region and (3) exhibit high recombination of photogenerated electron–hole thus hindering its visible light-driven photocatalytic performance [1, 12–19]. Thus, remarkable efforts have been devoted to overcome all these limitations by doping/composite with metal, non-metal (NPs), noble metal inclusion or deposition to gain plasmonic property [20–28] and etc. Among of them, doping with metal such as Ag/TiO_2, Au/TiO_2 and etc. is the best approaches for improving photocatalytic performance of TiO_2 [9]. Recently it was found that core–shell structures based MSO_4 (M = a metal) shell show significant optical properties and higher photocatalytic efficiency compared to single core. For example Fang and et al. [29] found that PbS coated with $PbSO_4$ leaded to remarkable optical properties. Herein, we have reported microwave-assisted synthesis of $Ag@Ag_2SO_4$ with SDS as a sulfur source and surfactant and our results showed that $Ag@Ag_2SO_4$ not only improve the optical properties of single-Ag but also promote the photocatalytic efficiency. To our knowledge, it is the first report for synthesis and characterization of $Ag@Ag_2SO_4$. Moreover, $Ag@Ag_2SO_4$ nanoparticles were utilized as co-photocatalyst for the photocatalytic degradation of methylene blue (MB). The prepared products were characterized extensively by means of XRD, TEM, SEM. FT-IR, and DRS.

✉ Zabihullah Zarghami
z.zarghami@ut.ac.ir

[1] Young Researchers and Elites Club, South Tehran branch, Islamic Azad University, Tehran, Iran

[2] Young Researchers and Elites Club, Arak Branch, Islamic Azad University, Arak, Iran

[3] Department of Chemistry, Arak Branch, Islamic Azad University, Arak, Iran

2 Experimental

2.1 Materials and characterization

All the chemical reagents were of analytical grade and were used as received without any further purification. The crystal structural and compositional properties of products were recorded by X-ray diffraction (Philips-X'PertPro) and FT-IR (Magna-IR, spectrometer 550 Nicolet with 0.125 cm^{-1} resolution in KBr pellets in the range of 400–4000 cm^{-1}). The XL30, Philips microscope set was used in order to investigate the energy dispersive spectrometry (EDS) analysis. The morphology of the obtained products was investigated by scanning electron microscopy (LEO-1455VP). The Philips EM208S transmission electron microscope with an accelerating voltage of 200 kV was applied in order for taking Transmission electron microscope (TEM) images. UV–Vis diffuse reflectance spectroscopy analysis was carried out using Shimadzu UV-2600 UV–Vis spectrophotometer with an integrating sphere attachment and $BaSO_4$ was used as reference.

2.2 Synthesis of $Ag@Ag_2SO_4$

First of all, 0.05 gr $AgNO_3$ was dissolved in 5 mL of distilled water and 0.05 gr SDS was added. Afterwards, propylene glycol was added enough to bring the final volume of solution up to 40 mL. The obtained solution was microwave-heated at a power setting of 750 W for 1.5 min. Then, 0.02 mL hydrazine hydrate (20 %) was added to solution and was microwave-heated at a power setting of 750 W for 2.5 min. The microwave oven followed a working cycle of 30 s on and 30 s off. The obtained precipitate was collected (sample 1) and was characterized. To form $Ag@Ag_2SO_4$ (sample 2), the sample 1 was annealed at 350 °C for 1 h. The obtained product was washed with distilled water and ethanol for several times (sample 2).

2.3 Preparation of $Ag@Ag_2SO_4/TiO_2$

$Ag@Ag_2SO_4/TiO_2$ have been prepared by adding calculated amount (3.4×10^{21} atoms) of $Ag@Ag_2SO_4$ nanoparticles onto TiO_2 (25 mg) and stirring was done overnight followed by drying at 100 °C.

2.4 Photocatalysis experiments

In order to evaluate photocatalytic activity of the $Ag@Ag_2SO_4/TiO_2$, photocatalytic degradation of methylene blue (MB) dye was under taken. A typical experiment constitutes $Ag@Ag_2SO_4/TiO_2$ (20 mg) were added into a glass beaker containing of 150 mL of dye aqueous solution (5 mg/L in ethanol as solvent), and then dispersed by stirring for 30 min at 20–25 °C in darkness to establish adsorption–desorption equilibrium between the dye molecules and $Ag@Ag_2SO_4/TiO_2$ surface. Later, a series of UV lamps (6 × 15 W, Philips) were switched on a 20 cm distance over the suspension surface. Finally, the absorbance spectra of the methylene blue solution were recorded by a UV–Vis spectrophotometer (Shimadzu UV–Vis spectrometer) and the decolorization rate was calculated according to the absorbance change.

3 Results and discussion

Figure 1a, b show typical XRD patterns of synthesized Ag nanoparticles (sample 1) and $Ag@Ag_2SO_4$ nanostructures (sample 2). All the XRD diffraction peaks are indexed to cubic phase of Ag (JCPDS No. 87-0579, space group: Fm-3 m, with cell constant a = 4.0862 Å) and orthorhombic phase of Ag_2SO_4 (JCPDS No. 27-1403, space group: Fddd, with cell constant a = 10.2690, b = 12.7060 and c = 5.8181 Å). No crystalline impurity phases were observed in the products before and after annealing process (sample 1 and 2), indicating relatively high purity of Ag and $Ag@Ag_2SO_4$ nanostructures. The crystallite sizes of the samples 1 and 2 estimated by the Scherrer formula shown in Eq. 1 [30–33] are 21 and 34 nm, respectively.

$$D(hkl) = k\lambda/\beta\cos\theta \quad (1)$$

where D is the crystallite size, as calculated for the (hkl) reflection, λ is the wavelength of Cu Kα radiation (0.154178 nm), k is a constant related to the crystal shape (0.9), and β is the value of full width at half-maximum intensity (FWHM). Figure 2a, b show a typical EDX spectrum of unannealed (sample 1) and annealed (sample 2) products, respectively. Figure 2a shows that the pure silver nanoparticles have been synthesized. Moreover, the presence of Ag, S and O in Fig. 2b indicates that $Ag@Ag_2SO_4$ nanostructures have been obtained without any impurity. Figure 3a–c show SEM and TEM images of Ag and $Ag@Ag_2SO_4$ nanoparticles. According to Fig. 3a the morphology of the Ag nanoparticles obtained before annealing (sample 1), are sphere-like. Figure 3b shows the morphology of $Ag@Ag_2SO_4$ nanoparticles obtained after annealing (sample 2) that are sphere-like and the particles size are bigger than the obtained Ag nanoparticles (Fig. 3a). Figure 3c is TEM image of $Ag@Ag_2SO_4$ nanoparticles that shows the $Ag@Ag_2SO_4$ nanoparticles have been made of spherical core–shell nanoparticles with average particles size of 40–50 nm. Based on the Fig. 3c, the middle part of particles is darker which indicates the Ag core and the brighter part around these regions is a sign of

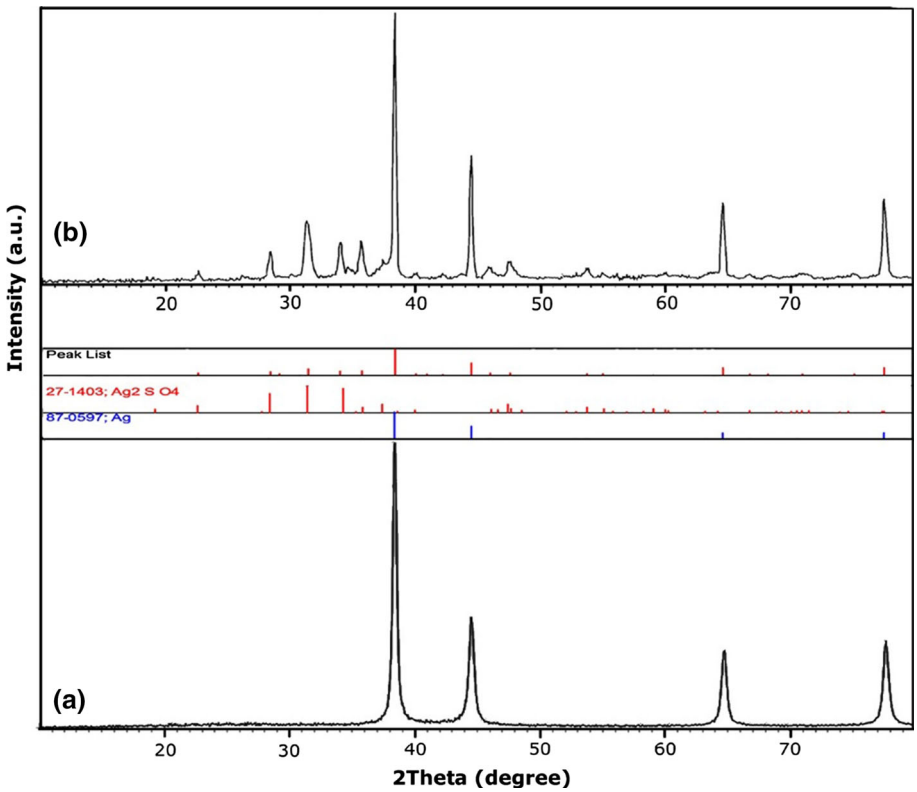

Fig. 1 XRD pattern of *a* Ag (sample 1) and *b* $Ag@Ag_2SO_4$ (sample 2) nanoparticle

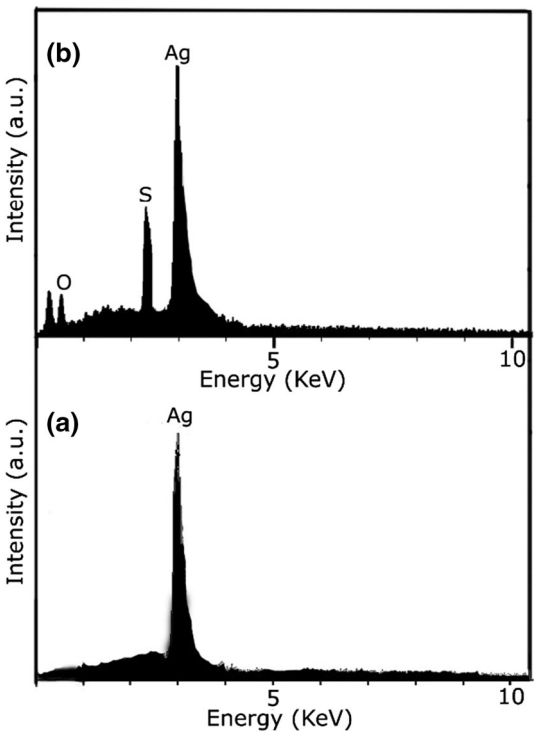

Fig. 2 EDX analysis of the as-synthesized product **a** Ag (sample 1) and **b** $Ag@Ag_2SO_4$ nanoparticles (sample 2)

Ag_2SO_4 shell thickness. The FT-IR spectra of samples 1 and 2 are shown in Fig. 4a, b, respectively. According to Fig. 4a, the weak peak as 3441 cm^{-1} is attributable to the v(OH) stretching which indicates the presence of physisorbed water molecules linked to Ag nanoparticles [34]. The two peaks at 2909 and 2841 cm^{-1} are related to the asymmetric and symmetric stretch vibrations of CH_2 group ascribe to the SDS [34]. Two peaks at 1619 and 972 cm^{-1} are attributed to the C–H groups [34]. Furthermore, the absorptions bonds at 1251 and 728 cm^{-1} are attributed to the S = O and CO–S bond, respectively [35]. So, Fig. 4a shows that there is SDS as a surfactant on the Ag nanoparticle surface. From FT-IR spectrum in Fig. 4b, The absorption bond at 1223 cm^{-1} can be allocated to the absorption band of S = O [35]. Moreover, the absorption peak at 536 cm^{-1} are attributed to Ag–O–SO_3 band. Figure 5a, b show absorption spectra of unannealed (Ag) and annealed ($Ag@Ag_2SO_4$) products. As can be seen, the absorption of annealed product is higher than unannealed product. It proves that the shell increases the absorption intensity. To evaluate the photocatalytic decomposition of MB, Ag/TiO_2, $Ag@Ag_2SO_4/TiO_2$ and TiO_2 were used as photocatalyst. Moreover, the photocatalytic decomposition was performed under UV-light illumination, and the degradation rate for the decomposition of MB was

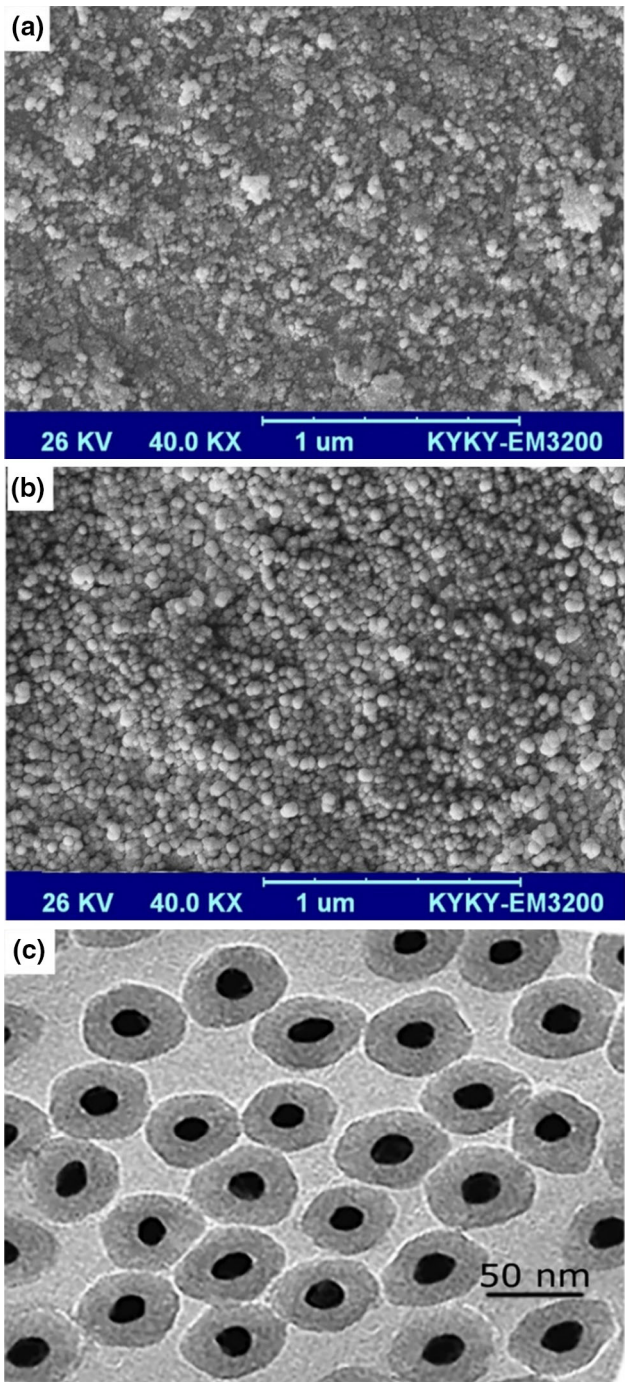

Fig. 3 SEM images of **a** Ag (sample 1) and **b** Ag@Ag_2SO_4 (sample 2), **c** TEM image of Ag@Ag_2SO_4 (sample 2)

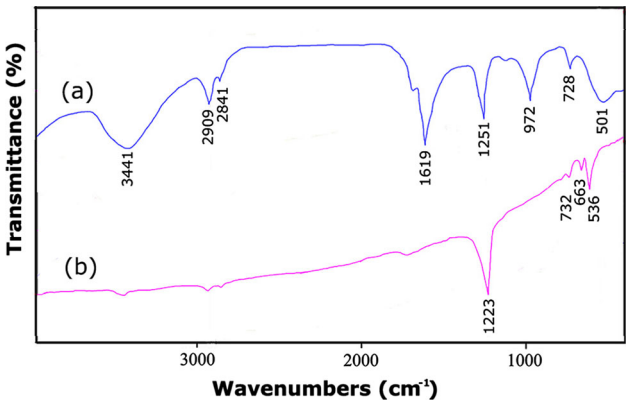

Fig. 4 FT-IR spectra of *a* Ag (sample 1) and *b* Ag@Ag_2SO_4 (sample 2)

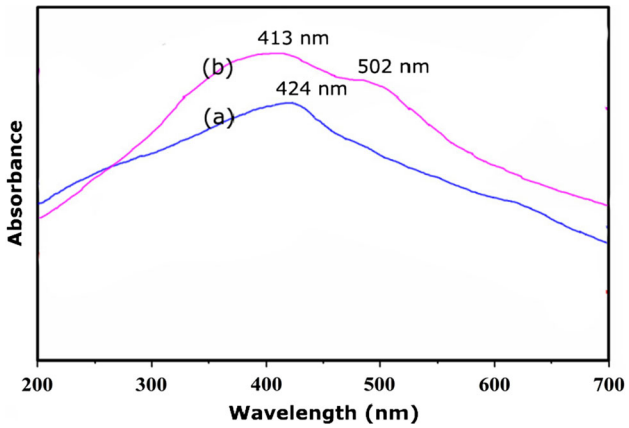

Fig. 5 Absorption spectra of *a* Ag and *b* Ag@Ag_2SO_4

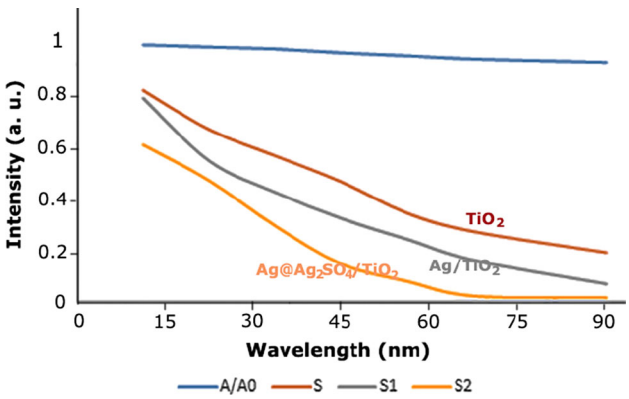

Fig. 6 Photodecolorization of methylene blue by blank, TiO_2, Ag and Ag@Ag_2SO_4 nanoparticles

estimated by observing the changes in absorbance (absorption intensity vs. irradiation time) obtained by UV–Vis spectra. Figure 6 exhibits the plot of the remaining dye concentration (A/A0) versus time intervals for the photocatalytic reaction of Ag/TiO_2, Ag@Ag_2SO_4/TiO_2 and TiO_2 nanoparticles. According to Fig. 4e, in absence of TiO_2, as-synthesized Ag and Ag@Ag_2SO_4 nanoparticles, almost negligible radiation of MB is observable (blue line). On the other hand, when utilizing the TiO_2, Ag/TiO_2, Ag@Ag_2SO_4/TiO_2 as the photocatalyst, it is estimated that 78, 89 and 99 % of MB is degraded under UV-light illumination after 90 min, respectively. As a result, shell causes an

increase in Ag nanoparticle photocatalyst efficiency of Ag. The reaction processes for synthesis Ag-core/Ag_2SO_4-shell nanoparticles can be described as follow:

$$N_2H_4 \rightarrow N_2 + 4H^+ + 4e^- \quad (2)$$

$$Ag^+ + e^- \rightarrow Ag \quad (3)$$

$$\text{Extra } Ag^+ + CH_3(CH_2)_{10}OSO_3 \rightarrow Ag_2{-}OSO_3(CH_2)_{10}CH_3 \quad (4)$$

$$Ag_2{-}OSO_3(CH_2)_{10}CH_3 \xrightarrow[350\,^\circ C\ 1h]{\text{annealing}} Ag_2SO_4 \quad (5)$$

4 Conclusion

Herein, for the first time, Ag-core/Ag_2SO_4-shell nanoparticles have been successfully synthesized via microwave-assisted route. Optical property investigation shows that the Ag_2SO_4-sheathed Ag nanoparticles have an intense luminescence in cyan region. According to the aforementioned results, the thin Ag_2SO_4 shell causes the prevention of further oxidation of Ag core effectively. It was found that Ag@Ag_2SO_4 nanoparticles have higher photocatalytic efficiency and MB degradation efficiency than Ag nanoparticles.

Acknowledgments This work was supported by the Chemistry Research Center at Islamic Azad University Arak.

References

1. K.H. Leong, P. Monash, S. Ibrahim, P. Saravanan, Sol. Energy **101**, 321 (2014)
2. E. Savinkina, G. Kuzmicheva, L. Obolenskaya, Int. J. Energy Environ. **6**, 268 (2012)
3. M. Mousavi-Kamazani, M. Salavati-Niasari, M. Sadeghinia, Mater. Lett. **142**, 145 (2015)
4. M. Panahi-Kalamuei, M. Mousavi-Kamazani, M. Salavati-Niasari, S.M. Hosseinpour-Mashkani, Ultrason. Sonochem. **23**, 246 (2015)
5. M. Panahi-Kalamuei, M. Mousavi-Kamazani, M. Salavati-Niasari, Mater. Lett. **136**, 218 (2014)
6. M. Panahi-Kalamuei, F. Mohandes, M. Mousavi-Kamazani, M. Salavati-Niasari, Z. Fereshteh, M. Fathi, Mater. Sci. Semicond. Process. **27**, 1028 (2014)
7. Y. Zhao, L. Kuai, B. Geng, Catal. Sci. Technol. **2**, 1269 (2012)
8. P. Christensen, T. Curtis, T. Egerton, S. Kosa, J. Tinlin, Appl. Catal. B Environ. **41**, 371 (2003)
9. A. Stoyanova, M. Sredkova, R. Iordanova, Y. Dimitriev, A. Bachvarova-Nedelcheva, Adv. Mater. **4**, 2059 (2010)
10. K. Zhao, Y. Lu, N. Lu, Y. Zhao, X. Yuan, H. Zhang, L. Teng, F. Li, Appl. Surf. Sci. **285**, 616 (2013)
11. Y. Tang, Z. Jiang, Q. Tay, J. Deng, Y. Lai, D. Gong, Z. Dong, Z. Chen, RSC Adv. **2**, 9406 (2012)
12. W. Cui, H. Wang, L. Liu, Y. Liang, J.G. McEvoy, Appl. Surf. Sci. **283**, 820 (2013)
13. A. Ramchiary, S. Samdarshi, Appl. Surf. Sci. **305**, 33 (2014)
14. A. Bumajdad, M. Madkour, Phys. Chem. Chem. Phys. **16**, 7146 (2014)
15. J. Yang, H. Bai, X. Tan, J. Lian, Appl. Surf. Sci. **253**, 1988 (2006)
16. J. Zhang, D. Fu, H. Gao, L. Deng, Appl. Surf. Sci. **258**, 1294 (2011)
17. S.T. Kochuveedu, Y.H. Jang, D.H. Kim, Chem. Soc. Rev. **42**, 8467 (2013)
18. X. Zhou, G. Liu, J. Yu, W. Fan, J. Mater. Chem. **22**, 21337 (2012)
19. Z. Chen, L. Fang, W. Dong, F. Zheng, M. Shen, J. Wang, J. Mater. Chem. A **2**, 824 (2014)
20. Q. Xiang, J. Yu, M. Jaroniec, Phys. Chem. Chem. Phys. **13**, 4853 (2011)
21. Q. Xiang, J. Yu, W. Wang, M. Jaroniec, Chem. Commun. **47**, 6906 (2011)
22. J. Yu, Q. Xiang, M. Zhou, Appl. Catal. B Environ. **90**, 595 (2009)
23. J. Yu, L. Qi, M. Jaroniec, J. Phys. Chem. C **114**, 13118 (2010)
24. J. Yu, J. Xiong, B. Cheng, S. Liu, Appl. Catal. B Environ. **60**, 211 (2005)
25. W. Hou, Z. Liu, P. Pavaskar, W.H. Hung, S.B. Cronin, J. Catal. **277**, 149 (2011)
26. H. Zhang, X. Fan, X. Quan, S. Chen, H. Yu, Environ. Sci. Technol. **45**, 5731 (2011)
27. P. Wang, B. Huang, X. Qin, X. Zhang, Y. Dai, J. Wei, M.H. Whangbo, Angew. Chem. Int. Ed. **47**, 7931 (2008)
28. F. Xiao, J. Mater. Chem. **22**, 7819 (2012)
29. Z. Fang, X. Lin, Y. Fan, Y. Liu, Y. Ni, X. Wei, J. Alloys Compd. **493**, L25 (2010)
30. M. Mousavi-Kamazani, M. Salavati-Niasari, Compos. Part B Eng. **56**, 490 (2014)
31. M. Mousavi-Kamazani, M. Salavati-Niasari, M. Sadeghinia, Superlattice Microstruct. **63**, 248 (2013)
32. M. Mousavi-Kamazani, M. Salavati-Niasari, M. Ramezani, J. Clust. Sci. **24**, 927 (2013)
33. M. Mousavi-Kamazani, M. Salavati-Niasari, H. Emadi, Mater. Res. Bull. **47**, 3983 (2012)
34. M. Salavati-Niasari, S. Alizadeh, M. Mousavi-Kamazani, N. Mir, O. Rezaei, E. Ahmadi, J. Clust. Sci. **24**, 1181 (2013)
35. M. Salavati-Niasari, M. Ranjbar, F. Mohandes, Micro. Nano Lett. **7**, 581 (2012)